Carbohydrate Polymers 87 (2012) 1779–1786

Contents lists available at SciVerse ScienceDirect

Carbohydrate Polymers

journal homepage: www.elsevier.com/locate/carbpol

UV-initiated crosslinking of electrospun poly(ethylene oxide) nanofibers with pentaerythritol triacrylate: Effect of irradiation time and incorporated cellulose nanocrystals

Chengjun Zhou[a], Qingwen Wang[b], Qinglin Wu[a,*]

[a] School of Renewable Natural Resources, Louisiana State University Agriculture Center, Baton Rouge, LA 70803, USA
[b] Material Science and Engineering College, Northeast Forestry University, 26 Hexing Road, Harbin 150040, China

ARTICLE INFO

Article history:
Received 13 August 2011
Received in revised form
14 September 2011
Accepted 30 September 2011
Available online 6 October 2011

Keywords:
UV irradiation
Photo-crosslinking
Electrospinning
Nanofibers
Polyethylene oxide (PEO)
Cellulose nanocrystals (CNCs)

ABSTRACT

UV-initiated crosslinking of electrospun poly(ethylene oxide) (PEO) nanofibers in the presence of cellulose nanocrystals (CNCs) was performed with pentaerythritol triacrylate (PETA) as both photo-initiator and crosslinker in order to determine the effect of irradiation time and incorporated CNCs. The chemical structure and morphologies, swelling and mechanical properties of crosslinked nanofibers were investigated. The experimental results show that UV irradiation did not exhibit a dramatic effect on the diameter of PEO nanofibers. Among the irradiation time used, a 40 min time was optimal for the UV-initiated crosslinking process. With increased CNC content up to 10 wt%, the crosslinked PEO/CNC composite nanofibers became more uniform and smaller in diameter, and also showed a significant improvement in the swelling and mechanical properties. At the CNC content of 10 wt%, the maximum tensile stress and Young's modulus of the crosslinked PEO/CNC composite fibrous mats increased by 377.5 and 190.5% than those of uncrosslinked PEO mats, and 76.5 and 127.4% than those of crosslinked PEO mats, respectively.

1. Introduction

Polyethylene oxide (PEO) is a nontoxic, hydrophilic and biocompatible polymer, and thus has attracted tremendous attention in the biomedical field, especially in developing the scaffolds for tissue engineering and the matrix system for controlled drug release (Im, Bai, & Lee, 2010; Jin, Fridrikh, Rutledge, & Kaplan, 2002; Rahman, Khan, & Tareq, 2010). Since PEO is highly soluble in water, various methods such as electron beam (Merrill, Dennison, & Sung, 1993), gamma (γ)(Stringer & Peppas, 1996), and Ultraviolet (UV) irradiation (Doytcheva et al., 1997; Doytcheva, Stamenova, Zvetkov, & Tsvetanov, 1998) have been employed to crosslink PEO in order to prevent the dissolution and flow of PEO into the external medium. Among these methods, UV-induced crosslinking exhibits many advantages including easy manipulation and low hazard for the researchers, and highly effective and controllable reaction (Wang, Kempen, et al., 2008; Wang, Yaszemski, Gruetzmacher, & Lu, 2008; Wang, Yaszemski, Knight, Gruetzmacher, Windebank, & Lu, 2009). More importantly, the sterilization and crosslinking could be conducted simultaneously during the UV irradiation, which greatly facilitates the utilization of UV-induced crosslinking techniques for biomaterial preparations. During the past ten years, UV-induced crosslinking of PEO in the presence of pentaerythritol triacrylate (PETA) have been researched broadly because that PETA could act as both an initiator and a crosslinker while UV irradiation for PEO in both solution and solid state (Doytcheva, Dotcheva, Stamenova, & Tsvetanov, 2001). PEO crosslinked by PETA still showed the excellent biocompatibility, and thus has been used in biomedical applications such as drug delivery (Dimitrov, Dotcheva, & Lambov, 2004; Petrov et al., 2006), and the substrates for cell (Lensen et al., 2007) or protein absorption (Leung, Hitchcock, Brash, Scholl, & Doran, 2010) studies.

As one of the most versatile techniques for fabricating ultrafine polymer nanofibers, electrospinning has been becoming increasingly popular because its features of simplicity and cost-effectiveness (Greiner & Wendorff, 2007; Reneker & Yarin, 2008). The obtained electrospun nanofibers have a variety of interesting characteristics such as small diameter, large specific surface areas, and wide-range porosity (Lu, Wang, & Wei, 2009). When nanofibers based on water-soluble polymers are crosslinked, they only swell in an aqueous solution and then forming the hydrogels. Therefore, the crossliked nanofibers showed not only the improvement in mechanical properties, thermal stability, and solvent resistance, but also the rapid response or maximum interaction with the external environment because the molecular species through nanofibers

* Corresponding author. Tel.: +1 225 578 8369; fax: +1 225 578 4251.
E-mail address: wuqing@lsu.edu (Q. Wu).

0144-8617/$ – see front matter © 2011 Elsevier Ltd. All rights reserved.
doi:10.1016/j.carbpol.2011.09.095

or nanofibrous hydrogels is much faster than that of macroscopic matter or hydrogels (Gestos, Whitten, Spinks, & Wallace, 2010), which are demanded for many applications including but not limited to tissue-engineering scaffolds, drug delivery, actuators, and sensors (Shin, Spinks, Shin, Kim, & Kim, 2009; Zeng, Hou, Wendorff, & Greiner, 2005). Over the past few years, a large number of studies have been done on electrospun PEO nanofibers to investigate the effects of process conditions and solution compositions (Deitzel, Kleinmeyer, Harris, & Tan, 2001; Son, Youk, Lee, & Park, 2004; Theron, Zussman, & Yarin, 2004). However, the electrospun PEO nanofibers crosslinked by UV irradiation has not been fully investigated.

In our recent work, cellulose nanocrystals (CNCs), a non-toxic, biocompatible, and biodegradable nanofillers, were successfully incorporated into PEO nanofibers through the electrospinning process, and it was found that the CNCs effectively enhanced the mechanical properties of nanofibers (Zhou, Chu, Wu, & Wu, 2011). Moreover, CNCs also showed the obvious reinforcement for the water-soluble polymer even in high humidity environments (Peresin et al., 2010) or hydrogels state (Zhou, Wu, Yue, & Zhang, 2011; Zhou, Wu, & Zhang, 2011).

In this paper, UV-initiated crosslinking of electrospun PEO nanofibers in the presence of PETA was first performed to distinguish appropriate irradiation time for the fabrication of PEO nanofibers with desired properties. The CNC-incorporated PEO nanofibers with different CNC contents were also prepared and UV-irradiated. The chemical structure and morphologies, swelling and mechanical properties of crosslinked nanofibers were investigated. The goal of the study was to develop crosslinked composite nanofibers with high surface area combined by excellent mechanical and solvent resistant properties through UV irritations used as biomimetic materials for their potential applications in tissue engineering scaffolds and drug delivery.

2. Experimental

2.1. Raw materials

PEO with a viscosity molecular weight (M_v) of 900,000 g mol^{-1} and PETA were purchased from Sigma–Aldrich Inc. (St. Louis, MO, United States). Cotton-based CNCs were isolated from cotton fabrics (provided by the USDA ARS Southern Regional Research Center in New Orleans, LA, United States) by combined acid hydrolysis with 64% H_2SO_4 and high pressure homogenization process as described in our previous papers (Zhou, Wu, Yue, et al., 2011). The manufactured CNCs had a rod-like shape with a diameter of 8.7 ± 1.7 nm and a length of 70 ± 34 nm. The aqueous solutions/suspensions in all experiments were prepared with distilled water.

2.2. Electrospinning process

A certain amount of powder PEO was added into distilled water or fresh CNC suspension to obtain 5 wt% of PEO polymer solution/suspensions. The CNC loading percentage in relation to PEO weight was chosen as 0, 5, 10, and 20 wt%. The resulting mixtures were kept under vigorous magnetic stirring overnight at room temperature to obtain homogeneous pure PEO solution or PEO/CNC suspensions. PETA of 10 wt% with respect to PEO weight was added, and then the solution or suspension was further stirred vigorously for 1 h to dispense PETA under shading. The obtained solutions or suspensions were loaded into a 5-mL BD^{TM} plastic syringe with a 20 gauge (inner diameter = 0.584 mm) stainless steel needle. The needle was connected to a high voltage power supply (Gamma High Voltage Research, Inc., Ormond Beach, FL, United States), which generates positive DC voltages up to 30 kV. The flow rate of the solution/suspensions was controlled by a Chemyx Fusion 100 syringe pump (Stafford, TX, United States). A piece of grounded aluminum foil was placed under the capillary needle tip as a collector. The electrospinning parameters included a 15 kV voltage, a distance of 20 cm from needle tip to collector (equivalent to an electric field strength of 0.75 kV cm^{-1}), and a flow rate of 0.6 mL h^{-1}. To obtain test samples with structures matched as much as possible, all electrospun nanofibrous mats were produced from 3 mL of the corresponding electrospinning solution/suspensions with the spinning conditions stated above at 60% relative humidity and 25 °C. The obtained mats were vacuum-dried at 40 °C for 12 h, and then stored in a desiccator prior to characterization. The samples were designated as PEO–PETA or PEO/CNCy-PETA, where y (wt%) is the concentration of CNCs.

2.3. UV irradiation

The irradiation of mats was carried out by a SpectrolineSB-100P Super-High-Intensity UV Lamp (Spectronics Corporation, Westbury, NY, United States) emitted a light intensity of 4800 μW cm^{-2} at a wavelength of 365 nm at room temperature. The square mat samples of 40 mm were placed under UV light with a distance of around 4 cm from the lamp head. To avoid oxygen quenching, the irradiation was carried out under a constant flow of nitrogen. The irradiation time was designated as the total duration of irradiation subtracting 5 min because the initial 5-min time period is necessary for reaching the standard emission of the UV lamp.

2.4. Measurement and characterization

Conductivity of the electrospinning solutions was determined at room temperature using a Jenway Model 4330 conductivity & PH meter (Bath, United Kingdom). Shear viscosities of the solutions were measured using an AR2000ex Rheometer (TA Instruments Inc., New Castle, DE, United States). A 40-mm cone-plate geometry with a cone angle of 1°59′42″ and a truncation of 56 μm was used for the flow measurements. The temperature of test samples was kept at 25 °C with a Peltier device, and the shear rate was varied from 0.1 to 100 s^{-1}. To avoid the evaporation of water in the sample, the 56 μm gap between cone and parallel plate was sealed with a solvent trap cover, and the moat on the top of the cover was filled with low viscosity silicon oil.

Fourier transform infrared (FTIR) spectra of electrospun mats were measured using a Bruker FTIR analyzer (Tensor-27, Bruker Optics Inc., Billerica, MA, United States) with attenuated total reflectance (ATR) mode. Each spectrum was acquired in a transmittance mode on a Zn/Se ATR crystal cell by accumulation of 64 scans with a resolution of 4 cm^{-1} and a spectral range of 4000–600 cm^{-1}. Differential scanning calorimetry (DSC) measurements were performed with a TA Q200 system (TA Instruments Inc., New Castle, DE, United States) at a 10 °C min^{-1} heating rate from 5 °C to 110 °C in a 50 mL min^{-1} dynamic nitrogen atmosphere. Samples of 5 ± 0.5 mg were loaded into DSC pans sealed using a crimping tool. Field emission scanning electron microscopy (FESEM, a FEI Quanta 3D FEG dual beam SEM/FIB system, Hillsboro, Oregon, United States) was used to investigate surface morphologies of mats sputter-coated with gold for 2 min. The average diameter of the fibers was measured by the analysis of SEM images using the Adobe Photoshop software (Version CS2). One hundred nanofibers were randomly selected from each image and measured using the ruler tool. The equilibrium swelling ratio (ES, g/g) and gel fraction (GF, %) of UV crosslinked mats were measured in distilled water at room temperature. Dry rectangle samples of 10 mm length and 5 mm width with an initial weight (W_1) were immersed in a glass jar with excess distilled water (approximately 30 mL) for 72 h, then removed from the

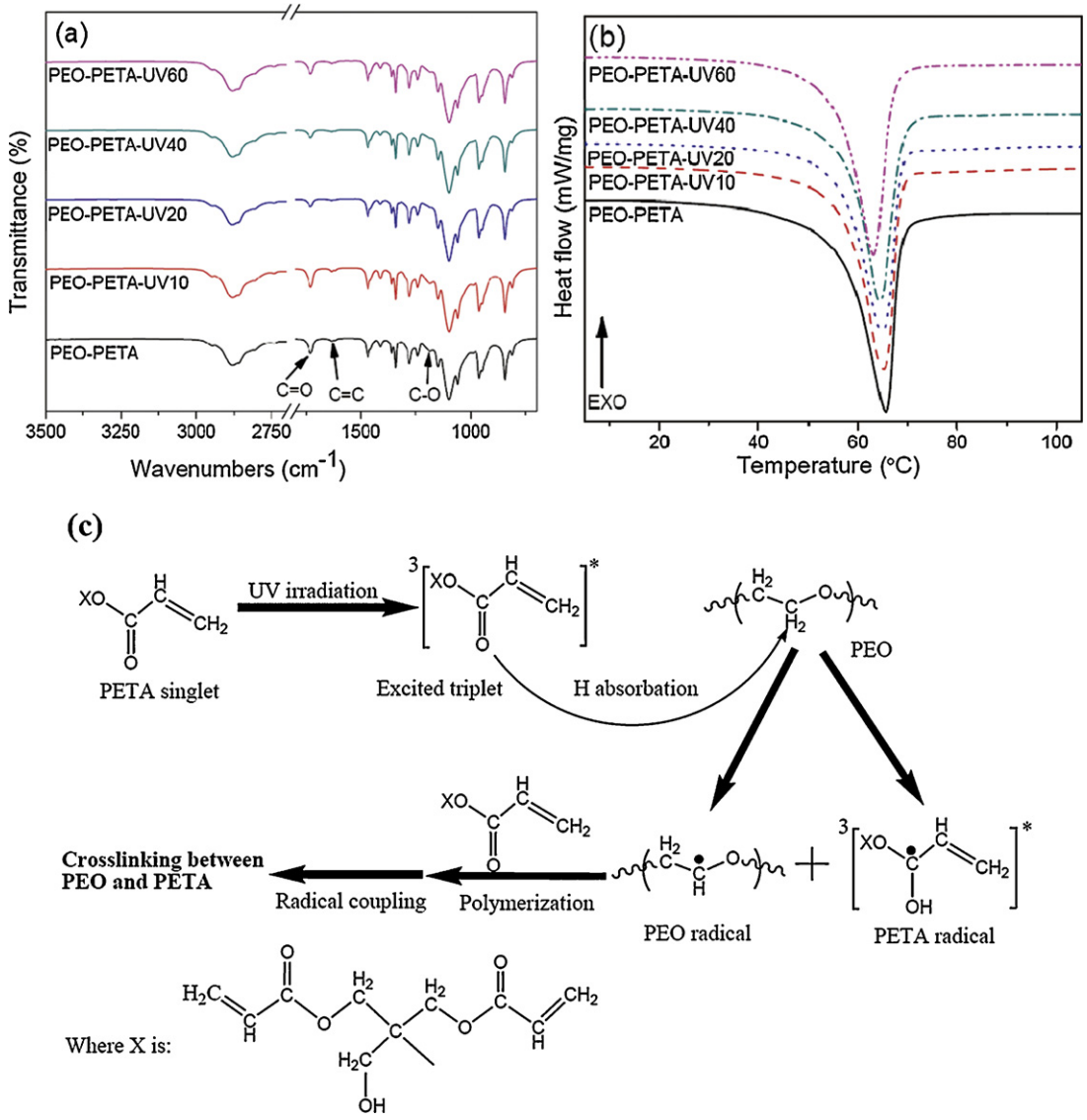

Fig. 1. FTIR spectra (a) and DSC curves (b) of electrospun PEO–PETA nanofibrous mats with different UV irradiation times, and (c) a schematic drawing showing possible crosslinking mechanism of PEO and PETA under UV irradiation.

solvent. The attached water on the surface of hydrogels was blotted with filter paper, and the weight of hydrogels (W_2) was measured. Five replicates were performed for each composition. The hydrogels at the equilibrium swelling state were extracted by isopropanol and dried in a vacuum oven for 12 h at 40 °C and re-weighed (W_2). ES and GF were calculated using the following equation:

$$\mathrm{ES} = \frac{W_2 - W_3}{W_3} \quad (1)$$

$$\mathrm{GF} = \frac{100 W_3}{W_1} \quad (2)$$

Mechanical properties of the nanofibrous mat samples (20 mm in length and 5 mm in width) were measured using an AR2000ex Rheometer with a solid clamp in tension mode at a 10 mm gauge length and a loading rate of 4.8 mm min^{-1} at room temperature. The thickness of the mats was measured using a Mitutoyo digimatic indicator with ±1 μm accuracy. Young's modulus for each sample was calculated from the initial linear portion of stress–strain curves through a linear regression analysis. Five replicates were performed for each composition.

3. Results and discussion

3.1. Effect of irradiation time

To elucidate the effect of UV irradiation time on the crosslink reaction, electrospun PEO–PETA nanofibers were investigated by FTIR (Fig. 1a) and DSC (Fig. 1b). From Fig. 1a, PEO–PETA nanofibers without irradiation, compared to pure PEO nanofibers (Zhou, Chu, et al., 2011), had three additional characteristic absorbance peaks (i.e., the C=O stretching at 1729 cm^{-1}, the C=C stretching at 1635 cm^{-1}, and the C–O stretching at 1183 cm^{-1}), which are attributed to PETA. This indicated that PETA was not selectively excluded during the electrospinning process. With the increase of UV irradiation time, the intensities of the three peaks decreased gradually, suggesting the UV photo-initiating and photo-crosslinking ability of PETA through the photo-initiation of C=O bond and then the polymerization of C=C bond (Doytcheva et al., 2001). Under UV irradiation, PETA could form an excited triplet state, and then absorb a proton from PEO chain and cleave C=O bond of PETA to form a PEO radical and a PETA radical, respectively. PEO radical produced attacks the C=C bond of PETA to initiate the polymerization of PETA. These obtained chains are terminated

through radical coupling to form the crosslinking between PEO and PETA. The possible mechanism for UV-initiated crosslinking between PEO and PETA is displayed in Fig. 1c. Interestingly, the three peaks became weaker at 20 and 40 min of irradiation time, which likely represents the optimization of the photo-crosslinking for PEO–PETA nanofibers. Fig. 1b shows DSC curves of crosslinked PEO–PETA nanofibers at different irradiation times. The thermal parameters, including melting temperatures (T_m), enthalpy of fusion (ΔH_m), and weight fractional crystallinities (X'_C, the degree of crystallinity of the PEO in the composites), were measured from the DSC curves and the corresponding data are summarized in Table 1. As shown in Fig. 1 and Table 1, T_m and X'_C of the irradiated PEO–PETA nanofibers are lower than those of their unirradiated counterparts, suggesting the existence of crosslinked reaction between PEO and PETA because crystallites can be prohibited by crosslinks (Wang, Yaszemski, et al., 2008). As the irradiation time increased, all the thermal parameters of PEO–PETA decreased gradually. More importantly, a 40 min UV irradiated time was optimal for the crosslinking process among the irradiation times used because its crystallinities were the lowest.

The effect of UV irradiation time on the swelling properties of PEO–PETA nanofibers is shown in Fig. 2. With an increase of irradiation time, the equilibrium swelling ratio gradually decreased. This behavior indicates that longer irradiation time increased the crosslink density of the PEO fibers. It can also be observed that gel fraction of mats first increased with increased irradiation time from 0 to 40 min and then slightly decreased. The results indicated an increased soluble part of PEO fibers above 40 min likely attributed to the photo-degradation of PEO (Vijayalakshmi & Madras, 2006), which is in agreement with the results of FTIR and DSC above.

Fig. 3 shows the morphology of electrospun PEO–PETA nanofibrous mats without and with UV irradiation. The diameters

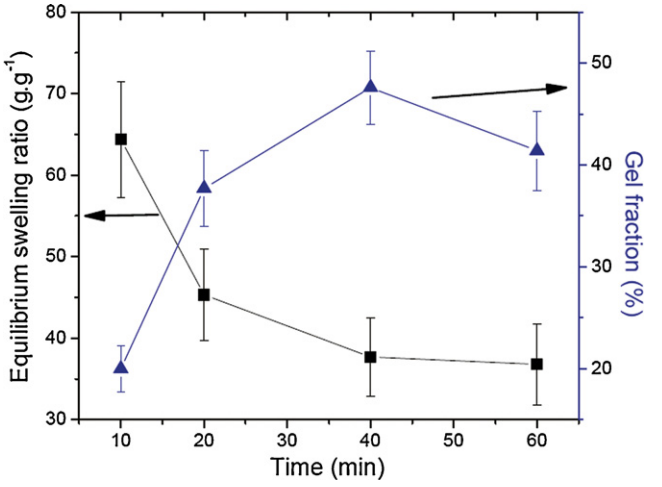

Fig. 2. Swelling properties of electrospun PEO–PETA nanofibrous mats with the different UV irradiation times. The standard deviations shown as error bars are based on five replicated samples.

are 257 ± 76 nm for PEO–PETA and 244 ± 45 nm for UV treated PEO–PETA nanofibers. It suggests that exposure of PEO nanofibers to UV irradiation did not exhibit a significant effect on nanofiber diameters. However, it can be found that the surface of nanofibers became rougher after UV irradiation from Fig. 3b and d. As PETA tended to segregate to the surface of PEO matrix (Leung et al., 2010), the photo-crosslinking reaction between PETA and PEO mostly occurred at the surface of PEO–PETA nanofibers, which resulted in the severe contraction of nanofiber surface.

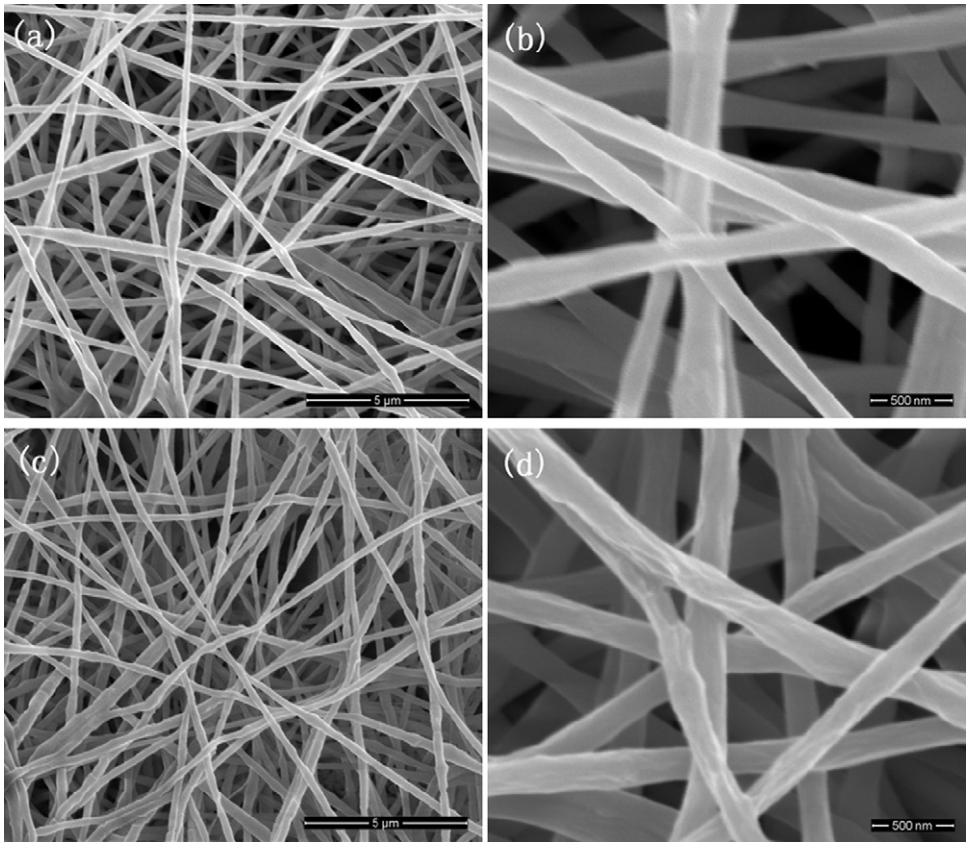

Fig. 3. SEM micrographs of PEO–PETA nanofibers without UV irradiation (a: 10,000×; b: 50,000×), and PEO–PETA nanofibers with UV irradiation for 40 min (c: 10,000×; d: 50,000 ×).

Table 1
The thermal properties of PEO–PETA nanofibrous mats with different CNC contents.

Sample	T_m (°C)	ΔH_m (J g^{-1})	X'_C (%)[a]
Pristine PEO–PETA	65.7	153.7	82.5
PEO–PETA–UV10	65.1	147.7	79.3
PEO–PETA–UV20	64.7	139.9	75.1
PEO–PETA–UV40	64.4	136.8	73.4
PEO–PETA–UV60	63.1	138.7	74.4
PEO/CNC5–PETA	67.4	136.2	76.4
PEO/CNC10–PETA	66.5	132.7	77.7
PEO/CNC20–PETA	65.2	116.8	74.1

[a] X'_C was calculated using equation of X'_C (%) $= 100 \times (\Delta H_m / C_{PEO} \Delta H^0)$, where $\Delta H^0 = 205$ J g^{-1} is the enthalpy of fusion of 100% crystalline PEO, C_{PEO} is the weight fraction of the PEO matrix in the composite.

Since a 40-min irradiation time was optimal for the UV-initiated crosslinking of PEO–PETA based on the above discussion, all electrospun PEO–CNC nanofibrous mats with different CNC contents reported later in this paper were UV irradiated for 40 min.

3.2. Effect of CNC content

Fig. 4a shows measured viscosity of PEO solution and PEO/CNC suspensions in the presence of PETA under different shear rates. The viscosity curve of PEO–PETA solution displayed two distinctive regions. Within the shear rate range from 0.1 to about 1.0 s^{-1}, a Newtonian fluid characteristic was observed. Then the viscosity of PEO–PETA solution sharply decreased with increased shear rate. In contrast, all the PEO/CNC–PETA suspensions exhibited a typical shear-thinning phenomenon through the whole range of shear rates from 0.1 to 100 s^{-1}, which was significantly different from the PEO–PETA solution. In addition, PEO/CNC–PETA suspensions exhibited more shear thinning behavior with increased CNC contents attributed to the enhanced solution inertia originating from the strong interaction between PEO and CNCs (Zhou, Chu, et al., 2011). More importantly, the increased viscosity for PEO/CNC–PETA suspensions is observed with the increase of CNC contents likely because the formed network structure of CNCs within the polymer solutions (Bercea & Navard, 2000). Fig. 4b shows the change in the conductivity of electrospinning PEO solution and PEO/CNC suspensions. With the increase of CNC contents, the significantly increased conductivity was observed. This behavior is because of the presence of uronic acid and sulfate ester groups on the CNC surface (Zhou, Wu, & Zhang, 2011), which promoted the formation of electrospun fibers with smaller diameter.

DSC was used to investigate the crosslinked PEO–PETA with different CNC contents, as shown in Table 1. After the addition of 5 wt% of CNCs, the melting temperature and degree of crystallinity of crosslinked PEO–CNC mats increased because CNCs acted as a nucleating agent for the crystallization of polymer matrix during electrospinning process. A similar effect was reported by Siqueira et al. for polycaprolactone reinforced with sisal cellulose whiskers (Siqueira, Bras, & Dufresne, 2009). However, with further increase in CNC content, T_m of crosslinked PEO/CNC mats decreased gradually. The same observation was reported for uncrosslinked PEO/CNC nanocomposites and ascribed to the formation of CNCs network within the matrix and the strong interactions between CNCs and PEO (Samir, Alloin, Sanchez, & Dufresne, 2004; Zhou, Chu, et al., 2011). It is worth noting that the addition of 10 wt% of CNCs induced the highest degree of crystallinity, likely suggesting that a close CNCs network began to form within the individual PEO fibers at the content of 10 wt% of CNCs. However, the excess CNCs can be regarded as the impurity for PEO and hinder the crystallization process of PEO chains.

Fig. 5 shows typical SEM images of crosslinked PEO/CNC nanofibers. The corresponding fiber diameter histograms are also given in Fig. 5. All fibers were homogeneous and exhibited decreased average diameters and diameter deviations from 244 ± 45 to 183 ± 22 nm with increased CNC content up to 10 wt% (Fig. 5d), suggesting that more uniform and finer composite nanofibers were fabricated by incorporating CNCs. This phenomena is similar to the results of electrospun PEO/CNC nanocomposite fibers without photo-crosslink in our previous report (Zhou, Chu, et al., 2011), and was attributed to the enhanced electric conductivity of electrospinning solutions in the presence of CNCs, as shown in Fig. 4b above. From Fig. 5c, the increased diameter and straighter shape for crosslinked PEO/CNC20-PETAnanofibers were observed. This behavior might be attributed to the unstable jet flow arising from the unbalanced forces among the surface tension, viscoelastic, and electrostatic forces. In general, a high concentration of electrospinning solutions could form the nanofibers with a larger and more uniform diameter because of its high viscoelastic behavior (Deitzel et al., 2001). While the enhanced electric conductivity for the electrospinning solutions could increase the charge density in ejected jets and the electrostatic forces, and thus induce the formation of straighter shape and smaller diameter of electrospun nanofibers (Son et al., 2004). When the effect of increased viscosity on the diameter of nanofibers is over that of enhanced electrical conductivity, the elongation of jet between the needle tip and the collector weakens. Therefore, the thick PEO/CNC–PETA nanofibers were obtained at the high CNC contents.

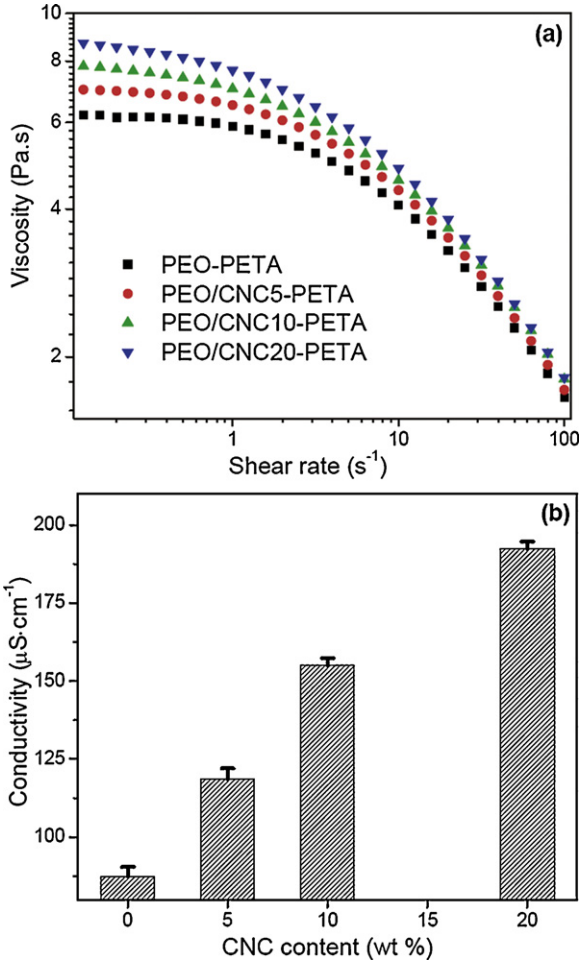

Fig. 4. Variations of apparent viscosity with shear rate (a) and conductivity with CNC content (b) of PEO–PETA solutions and PEO/CNC–PETA suspensions.

Fig. 6 shows the measured equilibrium swelling ratio and gel fraction for crosslinked PEO–PETA nanofibrous mats with different

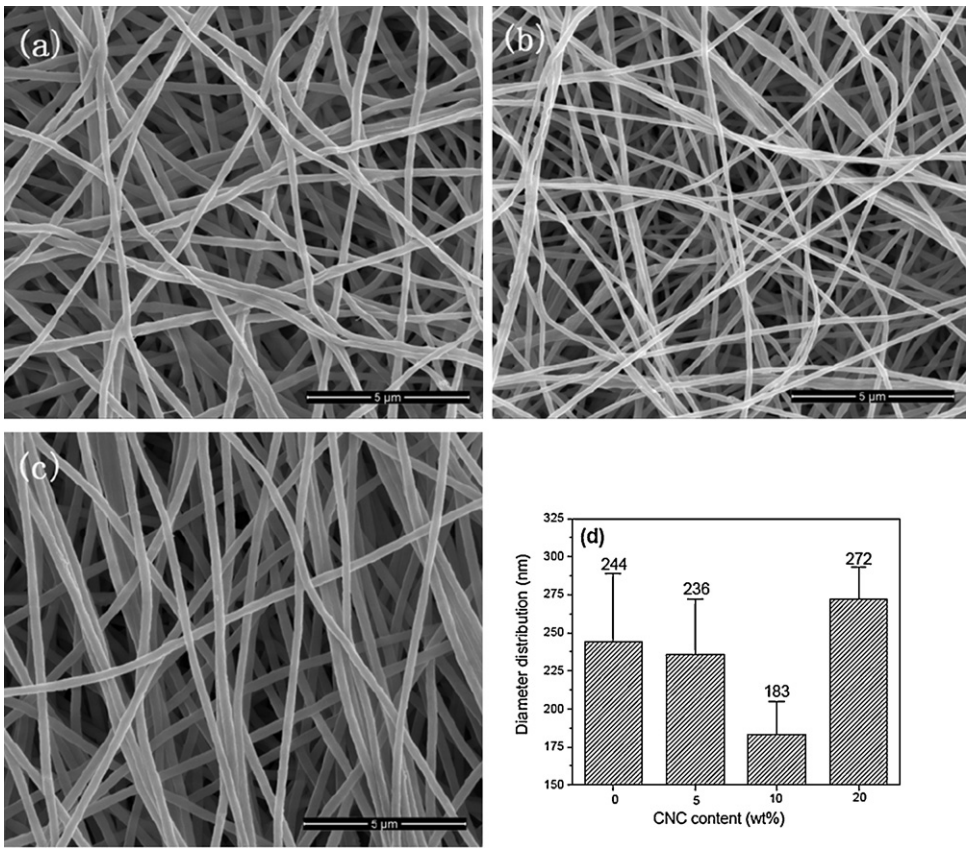

Fig. 5. SEM micrographs of crosslinked PEO/CNC5-PETA (a), PEO/CNC10-PETA (b), and PEO/CNC20-PETA (c) nanofibers at an electrical field strength of 0.75 kV cm^{-1} and a flow rate 0.6 mL h^{-1}; and the effect of CNC content on the diameter distribution of crosslinked PEO/CNC nanofibers (error bars show standard deviations based on randomly selected 100 fiber samples).

CNC contents. With an increase of the CNC content, the equilibrium swelling ratio of mats gradually decreased. Due to the fact that CNCs only absorbed little water but were insoluble in water (Zhou, Wu, Yue, et al., 2011), they could reduce the interactions between the water and crosslinked PEO networks and prohibit this networks from swelling in water. It was also observed that the gel fraction of crosslinkedPEO/CNC10-PETA mats increased to 55.1 from 47.6 of crosslinked PEO–PETA mats, likely because that the presence of CNCs immobilized PEO chain to dissolve in water. When CNC content was above the 10 wt% level, the gel fraction of mats showed a slightly decreasing trend with increased CNC contents. Lower gel fraction value indicated a higher soluble fraction attributed to the probable disturbance of a large amount of CNCs in the photo-crosslinking reaction. As observed in our recent reports (Zhou, Chu, et al., 2011), CNCs dispensed in PEO fibers had radial anisotropy or a skin-core morphology. The core had more nanocrystals but they were oriented more randomly, while the skin had fewer CNCs with a higher degree of orientation (Cai, Guinn, & Wang, 2011; Zhou, Wang, Zhang, Zhuang, & Han, 2008). As a result, higher loading of CNCs could become more compacted in the skin of PEO fibers and thus decreased the efficiency of photo-crosslink, which led to the smaller GF value of nanofibers.

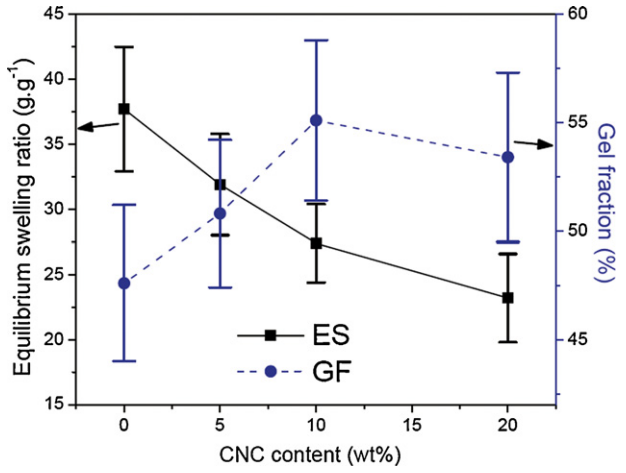

Fig. 6. Swelling properties of crosslinked PEO–PETA nanofibrous mats with different CNC contents. The standard deviations shown as error bars are based on five replicated samples.

Table 2 lists the mechanical properties of electrospun nanofibrous mats including the maximum tensile stress (σ_{max}), Young's modulus (E), and the elongation at break (ε_b). The uncrosslinked PEO nanofibrous mats had σ_{max} of 2.49 MPa, $E$of 13.7 MPa, and $\varepsilon_b$of 245%. After the photo-crosslinking, σ_{max} and E increased to 6.74

Table 2
Thickness and tensile properties of PEO–PETA nanofibrous mats with different CNC contents.

Sample	Thickness (μm)[a]	σ_{max} (MPa)	E (MPa)	ε_b (%)
Pristine PEO–PETA	40(5)	2.49(0.08)	13.7(0.7)	245(20)
PEO–PETA	39(4)	6.74(0.25)	17.5(1.1)	221(16)
PEO/CNC5–PETA	42(5)	8.73(0.30)	31.3(1.4)	201(12)
PEO/CNC10–PETA	44(6)	11.89(0.57)	39.8(1.9)	163(9)
PEO/CNC20–PETA	48(9)	14.22(0.78)	36.3(1.5)	167(10)

[a] The values in the parenthesis show standard deviation based on five replicated samples.

and 17.5 MPa (170.7 and 27.7% increase), respectively. This result indicated the UV-initiated crosslinking of PEO using PETA as an initiator and a crosslinker could significantly improve the mechanical properties of PEO nanofibrous mats. After the incorporation of CNCs into PEO nanofibers, σ_{max} and E of the crosslinked composite nanofibrous mats increased obviously, whereas ε_b decreased markedly, making mats much stronger and more resistant to deformation. In general, mechanical properties of electrospun composite nanofibrous mats are mainly influenced by their component properties, nanofiber structure, and the interaction among the nanofibers (Lee, Kim, Ryu, Kim, & Choi, 2003). From component properties, such reinforcements were attributed to the increase in the crystallinity induced by CNCs and the efficient stress transfer from PEO to CNCs through hydrogen bonding between these two components, which is in agreement with the results reported in CNCs reinforced poly(acrylic acid) (Lu & Hsieh, 2009). In addition, the decreased diameter of composite nanofibers was also benefited to the improved mechanical properties of mats because of tighter cohesion among the nanofibers composed of strong polar of PEO and CNCs (Huang, Zhang, Ramakrishna, & Lim, 2004). With increased CNC contents from 0 to 10 wt%, the values of σ_{max} and E of crosslinked mats increased by 76.5 and 127.4%, respectively, whereas ε_b decreased from 221 to 163%. With further increase of the CNC content, σ_{max} of crosslinked composite mats increased continually, but decreased E and increased ε_b were observed. Because the modulus E was determined from the initial linear portion in stress–strain curve, decreased E could be ascribed to the increased diameter of nanofibers (as shown in Fig. 5c above), resulting in the weakened interaction among nanofibers.

4. Conclusion

UV-initiated crosslinking of electrospun PEO nanofibers were successfully performed with PETA used as both initiator and crosslinker. UV irradiation did not exhibit a significant effect on the diameter of PEO–PETA nanofibers, and a 40-min irradiation time was optimal for the crosslinking process among the times used based on the results of DSC and swelling properties of PEO–PETA nanofibers. The crosslinked PEO–PETA nanofibers incorporated by CNCs became more uniform and smaller in diameter with increased CNC-loading up to the 10 wt% CNC content. The crosslinked PEO/CNC composite nanofibers showed the decreased swelling ratio and increased gel fraction with increased CNC contents. The crosslinked PEO/CNC composite nanofibers also exhibited a significant improvement in the mechanical properties attributed to the synergies of PEO crosslinking network and CNC's reinforcement. The maximum tensile stress and Young's modulus of crosslinked PEO/CNC10-PETA mats increased by 377.5 and 190.5% than those of uncrosslinked PEO–PETA mats, and 76.5 and 127.4% than those of crosslinked PEO–PETA mats, respectively. This study develops crosslinked composite nanofibers with smaller dimensions combined by excellent mechanical properties targeted for rapid response systems.

Acknowledgments

This work is financially supported by the Louisiana Board of Regents Industrial Tie Subprogram (Award number: LEQSF [2010–13]-RD-B-01), and the National Science Foundation of China (Award number: 31010103905).

References

Bercea, M. & Navard, P. (2000). Shear dynamics of aqueous suspensions of cellulose whiskers. *Macromolecules*, *33*(16), 6011–6016.

Cai, L., Guinn, A. S. & Wang, S. F. (2011). Exposed hydroxyapatite particles on the surface of photo-crosslinked nanocomposites for promoting MC3T3 cell proliferation and differentiation. *Acta Biomaterialia*, *7*(5), 2185–2199.

Deitzel, J. M., Kleinmeyer, J., Harris, D. & Tan, N. C. B. (2001). The effect of processing variables on the morphology of electrospun nanofibers and textiles. *Polymer*, *42*(1), 261–272.

Dimitrov, M., Dotcheva, D. & Lambov, N. (2004). Preparation and characterization of polyethylene oxide hydrogels with cytisine. *Acta Pharmaceutica Turcica*, *46*, 49–54.

Doytcheva, M., Dotcheva, D., Stamenova, R., Orahovats, A., Tsvetanov, C. & Leder, J. (1997). Ultraviolet-induced crosslinking of solid poly(ethylene oxide). *Journal of Applied Polymer Science*, *64*(12), 2299–2307.

Doytcheva, M., Dotcheva, D., Stamenova, R. & Tsvetanov, C. (2001). UV-initiated crosslinking of poly(ethylene oxide) with pentaerythritol triacrylate in solid state. *Macromolecular Materials and Engineering*, *286*(1), 30–33.

Doytcheva, M., Stamenova, R., Zvetkov, V. & Tsvetanov, C. B. (1998). UV irradiation-induced crosslinking of solid poly(ethylene oxide) modified with tetraalkyl ammonium salt. *Polymer*, *39*(26), 6715–6721.

Gestos, A., Whitten, P. G., Spinks, G. M. & Wallace, G. G. (2010). Crosslinking neat ultrathin films and nanofibres of pH-responsive poly(acrylic acid) by UV radiation. *Soft Matter*, *6*(5), 1045–1052.

Greiner, A. & Wendorff, J. H. (2007). Electrospinning: A fascinating method for the preparation of ultrathin fibres. *Angewandte Chemie-International Edition*, *46*(30), 5670–5703.

Huang, Z. M., Zhang, Y. Z., Ramakrishna, S. & Lim, C. T. (2004). Electrospinning and mechanical characterization of gelatin nanofibers. *Polymer*, *45*(15), 5361–5368.

Im, J. S., Bai, B. C. & Lee, Y. S. (2010). The effect of carbon nanotubes on drug delivery in an electro-sensitive transdermal drug delivery system. *Biomaterials*, *31*(6), 1414–1419.

Jin, H. J., Fridrikh, S. V., Rutledge, G. C. & Kaplan, D. L. (2002). Electrospinning Bombyx mori silk with poly(ethylene oxide). *Biomacromolecules*, *3*(6), 1233–1239.

Lee, K. H., Kim, H. Y., Ryu, Y. J., Kim, K. W. & Choi, S. W. (2003). Mechanical behavior of electrospun fiber mats of poly(vinyl chloride)/polyurethane polyblends. *Journal of Polymer Science Part B-Polymer Physics*, *41*(11), 1256–1262.

Lensen, M. C., Mela, P., Mourran, A., Groll, J., Heuts, J., Rong, H. T., et al. (2007). Micro and nanopatterned star poly(ethylene glycol) (PEG) materials prepared by UV-based imprint lithography. *Langmuir*, *23*(14), 7841–7846.

Leung, B. O., Hitchcock, A. P., Brash, J. L., Scholl, A. & Doran, A. (2010). An X-ray spectromicroscopy study of albumin adsorption to cross linked polyethylene oxide films. *Advanced Engineering Materials*, *12*(5), B133–B138.

Lu, P. & Hsieh, Y. L. (2009). Cellulose nanocrystal-filled poly(acrylic acid) nanocomposite fibrous membranes. *Nanotechnology*, *20*(41).

Lu, X. F., Wang, C. & Wei, Y. (2009). One-dimensional composite nanomaterials: Synthesis by Electrospinning and their applications. *Small*, *5*(21), 2349–2370.

Merrill, E. W., Dennison, K. A. & Sung, C. (1993). Partitioning and diffusion of solutes in hydrogels of poly(ethylene oxide). *Biomaterials*, *14*(15), 1117–1126.

Peresin, M. S., Habibi, Y., Vesterinen, A. H., Rojas, O. J., Pawlak, J. J. & Seppala, J. V. (2010). Effect of moisture on electrospun nanofiber composites of poly(vinyl alcohol) and cellulose nanocrystals. *Biomacromolecules*, *11*(9), 2471–2477.

Petrov, P., Bozukov, M., Burkhardt, M., Muthukrishnan, S., Muller, A. H. E. & Tsvetanov, C. B. (2006). Stabilization of polymeric micelles with a mixed poly(ethylene oxide)/poly(2-hydroxyethyl methacrylate) shell by formation of poly(pentaerythritol tetraacrylate) nanonetworks within the micelles. *Journal of Materials Chemistry*, *16*(22), 2192–2199.

Rahman, M. A., Khan, M. A. & Tareq, S. M. (2010). Preparation and characterization of polyethylene oxide (PEO)/gelatin blend for biomedical application: Effect of gamma radiation. *Journal of Applied Polymer Science*, *117*(4), 2075–2082.

Reneker, D. H. & Yarin, A. L. (2008). Electrospinning jets and polymer nanofibers. *Polymer*, *49*(10), 2387–2425.

Samir, M. A. S. A., Alloin, F., Sanchez, J. Y. & Dufresne, A. (2004). Cellulose nanocrystals reinforced poly(oxyethylene). *Polymer*, *45*(12), 4149–4157.

Shin, M. K., Spinks, G. M., Shin, S. R., Kim, S. I. & Kim, S. J. (2009). Nanocomposite hydrogel with high toughness for bioactuators. *Advanced Materials*, *21*(17), 1712–+.

Siqueira, G., Bras, J. & Dufresne, A. (2009). Cellulose whiskers versus microfibrils: Influence of the nature of the nanoparticle and its surface functionalization on the thermal and mechanical properties of nanocomposites. *Biomacromolecules*, *10*(2), 425–432.

Son, W. K., Youk, J. H., Lee, T. S. & Park, W. H. (2004). The effects of solution properties and polyelectrolyte on electrospinning of ultrafine poly(ethylene oxide) fibers. *Polymer*, *45*(9), 2959–2966.

Stringer, J. L. & Peppas, N. A. (1996). Diffusion of small molecular weight drugs in radiation-crosslinked poly(ethylene oxide) hydrogels. *Journal of Controlled Release*, *42*(2), 195–202.

Theron, S. A., Zussman, E. & Yarin, A. L. (2004). Experimental investigation of the governing parameters in the electrospinning of polymer solutions. *Polymer*, *45*(6), 2017–2030.

Vijayalakshmi, S. P. & Madras, G. (2006). Photocatalytic degradation of poly(ethylene oxide) and polyacrylamide. *Journal of Applied Polymer Science*, *100*(5), 3997–4003.

Wang, S. F., Kempen, D. H., Simha, N. X., Lewis, J. L., Windebank, A. J., Yaszemski, M. J., et al. (2008). Photo-cross-linked hybrid polymer networks consisting of poly(propylene fumarate) and poly(caprolactone fumarate): Controlled physical

properties and regulated bone and nerve cell responses. *Biomacromolecules*, *9*(4), 1229–1241.

Wang, S. F., Yaszemski, M. J., Gruetzmacher, J. A. & Lu, L. C. (2008). Photo-crosslinked poly(epsilon-caprolactone fumarate) networks: Roles of crystallinity and crosslinking density in determining mechanical properties. *Polymer*, *49*(26), 5692–5699.

Wang, S. F., Yaszemski, M. J., Knight, A. M., Gruetzmacher, J. A., Windebank, A. J. & Lu, L. C. (2009). Photo-crosslinked poly(epsilon-caprolactone fumarate) networks for guided peripheral nerve regeneration: Material properties and preliminary biological evaluations. *Acta Biomaterialia*, *5*(5), 1531–1542.

Zeng, J., Hou, H. Q., Wendorff, J. H. & Greiner, A. (2005). Photo-induced solid-state crosslinking of electrospun poly(vinyl alcohol) fibers. *Macromolecular Rapid Communications*, *26*(19), 1557–1562.

Zhou, C. J., Chu, R., Wu, R. & Wu, Q. L. (2011). Electrospun polyethylene oxide/cellulose nanocrystal composite nanofibrous mats with homogeneous and heterogeneous microstructures. *Biomacromolecules*, *12*(7), 2617–2625.

Zhou, C. J., Wang, S. F., Zhang, Y., Zhuang, Q. X. & Han, Z. W. (2008). In situ preparation and continuous fiber spinning of poly(p-phenylene benzobisoxazole) composites with oligo-hydroxyamide-functionalized multi-walled carbon nanotubes. *Polymer*, *49*(10), 2520–2530.

Zhou, C. J., Wu, Q. L., Yue, Y. Y. & Zhang, Q. G. (2011). Application of rod-shaped cellulose nanocrystals in polyacrylamide hydrogels. *Journal of Colloid and Interface Science*, *353*(1), 116–123.

Zhou, C. J., Wu, Q. L. & Zhang, Q. G. (2011). Dynamic rheology studies of in situ polymerization process of polyacrylamide-cellulose nanocrystal composite hydrogels. *Colloid and Polymer Science*, *289*(3), 247–255.